Supporting information for

The Role Played by Isopropyl Substiuents in Stabilizing the Putative Triple Bond in Ar'EEAr' (E=Si,Ge,Sn;Ar'=C_6H_3-2,6(C_6H_3-2,6-Pr^i_2)$_2$) and Ar*PbPbAr* (Ar*=C_6H_3-2,6(C_6H_2-2,4,6-Pr^i_3)$_2$)

Issaka Seidu, Michael Seth, Tom Ziegler[1]

Department of Chemistry, University of Calgary, 2500 University Dr. NW, Calgary, Alberta, Canada T2N 1N4

[1] **Email**: ziegler@ucalgary.ca

Linear ArEEAr. The NOCV deformation densities and contributing NOCV orbitals for the linear Si compound are illustrated in Figures S1 and S2,respectively, based on doublet fragments. Figure S1a displays the transfer of charge from the occupied $\tilde{\sigma}^*$ shown in Figure S2a as Ψ_{-1}^{α} to the empty $\tilde{\pi}^x$ bond shown in Figure S2a as Ψ_1^{α}. Figure S1a illustrates both the flow of the α-electron density $\Delta\rho_{orb}^{\sigma^*-\pi^x,\alpha}$ and the sum $\Delta\rho_{orb}^{\sigma^*-\pi^x} = \Delta\rho_{orb}^{\sigma^*-\pi^x,\alpha} + \Delta\rho_{orb}^{\sigma^*-\pi^x,\beta}$. The density change $\Delta\rho_{orb}^{\sigma^*-\pi^x}$ is associated with the formation of the π_{EE}^x orbital and the corresponding energy is -93.1 kcal/mol.

Figure S1b depict the π^y-bond formed by the movement of α-electron density ($\Delta\rho_{orb}^{\pi^y,\alpha}$) from the occupied π^y-orbital on the left side (orange) and an in-flow to the empty π^y-orbital on the right side (green). Also displayed in the figure is the sum $\Delta\rho_{orb}^{\pi^y}$ with a contribution of -37.4 kcal/mol. The NOCVs are given in Figure S2b.

Figure 9c displays the redistribution of charge ($\Delta\rho_{orb}^{\sigma-4s}$) from the $\tilde{\sigma}$ depicted in Figure 10c as Ψ_{-3}^{α} to the 4s orbitals on Si in both fragments shown in Figure S2c as Ψ_3^{α}. The sum of α and β contributions is also shown in Figure S1c. The density $\Delta\rho_{orb}^{\sigma-4s}$ corresponds to the formation of the σ_{EE} bond and the energy contribution is -26.3 kcal/mol.

The bonding picture observed here indicates that the linear Ar'SiSiAr' molecule has a triple bond, and the bond components and the corresponding energies are given in Table S1.

For linear Ar*PbPbAr* we observed one important bond component as it was in the case for the trans-bent system. Figure S3 represents the π^x-bond formed by the flow of α-electron density ($\Delta\rho_{orb}^{\pi^x,\alpha}$) from the occupied π^x-orbital on the right side (orange) and an in-flow to the empty π^x-orbital on the left side (green). Also depicted in the figure is the sum $\Delta\rho_{orb}^{\pi^x} = \Delta\rho_{orb}^{\pi^x,\alpha} + \Delta\rho_{orb}^{\pi^x,\beta}$ with a contribution of -28.2 kcal/mol. The results from our NOCV analysis of the linear ArEEAr systems are summarized in Table S2. The trends observed here are similar to those obtained for the trans-bent compounds.

Singlet triplet separation. For the linear geometry, E=Si and Ge revealed a singlet ground state with a negative singlet-triplet gap and no biradical character. However, a positive singlet-triplet gap was obtained for the E=Sn and E=Pb compounds. Thus, for these systems only two electron pairs are coupled with opposite spins in bonds whereas the third pair is coupled paramagnetically resulting in a triplet ground state. This is consistent with the small energy gap between the third and fourth frontier orbitals in Fig. 4. Table S3 displays the result for the SF calculations carried out on the linear compounds with the BP86 functional.

Biradical character. It follows from Table S6 that the ArEEAr systems have little biradical character for the singlet even in the linear conformation. Thus for all four elements the dominating contributions come from C_1 and C_2 with less than 5 % for diradical contributions.

Table S1. ETS[e] Analysis of the linear compounds carried out with the BP86 functional, energies in kcal/mol.

ArEEAr	ΔE_{Pauli}	ΔE_{elstat}	ΔE_{steric} [a]	ΔE_{orb}	ΔE_{disp}	ΔE_{int} [b]
Si[c]	253.4	-117.0	136.3	-166.3	-12.89	-42.9
Ge[c]	230.3	-117.0	113.3	-125.8	-14.15	-26.7
Sn[c]	171.0	-98.1	76.8	-81.2	-10.56	-18.9
Pb[d]	62.2	-35.2	27.0	-46.9	-10.16	-30.1

[a]Steric interaction energy, $\Delta E_{steric} = \Delta E_{Pauli} + \Delta E_{elstat}$.

[b]Total Interaction energy, $\Delta E_{\text{int}} = \Delta E_{steric} + \Delta E_{orb} + \Delta E_{disp}$.

[c]Ar'= C_6H_3-2,6(C_6H_3-2,6-iPr_2)$_2$.

[d]Ar*= C_6H_3-2,6(C_6H_2-2,4,6-iPr_3)$_2$.

[e]Based on doublet fragments.

Table S2. NOCV[d] Contributions to ΔE_{orb} [a] for the linear compounds carried out with the BP86 functional, energies in kcal/mol.

Compounds	$\Delta E_{orb}^{\pi^x}$	$\Delta E_{orb}^{\pi^y}$	$\Delta E_{orb}^{\sigma-4s}$	ΔE_{orb}^{rest}
Si[b]	-93.1	-37.4	-26.3	-5.3
Ge[b]	-63.8	-32.6	-18.9	-5.3
Sn[b]	-43.9	-15.5	-13.6	-5.5
Pb[c]	-28.2	--	--	-17.6

[a] $\Delta E_{orb} = \Delta E_{orb}^{\sigma-4s} + \Delta E_{orb}^{\pi^y} + \Delta E_{orb}^{\pi^x} + \Delta E_{orb}^{rest}$

[b]Ar'= C_6H_3-2,6(C_6H_3-2,6-iPr_2)$_2$.

[c]Ar*= C_6H_3-2,6(C_6H_2-2,4,6-iPr_3)$_2$.

[d]Based on doublet fragments.

Table S3. The singlet-triplet energy gap for the linear compounds carried out with the BP86 functional. Energies in eV.

Compounds	ΔE_{ST} [a] BP86
$Si_2Ar'_2$	-0.58
$Ge_2Ar'_2$	-0.11
$Sn_2Ar'_2$	0.20
$Pb_2Ar^*_2$	0.09

[a] The negative sign indicates that the singlet state is lower in energy than the triplet state and the positive sign (omitted) indicates that the triplet state is lower in energy than the singlet state.

Table S4. Contributions to the singlet [c] Ψ_{SF}^{S} wave function from a SF-CV(2)-DFT calculation on the trans-bent Ar'EEAr' (E=Si,Ge,Sn) and Ar*PbPbAr* sytems based on three local functionals.

	LDA			BLYP			BP86		
ArEEAr	[c] C_1	[c] C_2	C_3	C_1	C_2	C_3	C_1	C_2	C_3
Si[a]	0.9960	0.0015	0	0.9899	0.0040	0.0011	0.9868	0.0049	0.0014
Ge[a]	0.9963	0.0017	0	0.9922	0.0020	0.0017	0.9883	0.0052	0.0015
Sn[a]	0.9960	0.0007	0	0.9920	0.0032	0.0014	0.9869	0.0046	0.0026
Pb[b,c]	0.0063	0.9919	0	0.0103	0.9865	0.0007	0.0169	0.9771	0.0010

[a] Ar'= C_6H_3-2,6(C_6H_3-2,6-iPr_2)$_2$.

[b] Ar*= C_6H_3-2,6(C_6H_2-2,4,6-iPr_3)$_2$.

[c] See eq (19)

Table S5. Contributions to the singlet [c] Ψ_{SF}^{S} wave function from a SF-CV(2)-DFT calculation on the trans-bent Ar'EEAr' (E=Si,Ge,Sn) and Ar*PbPbAr* sytems based on two hybride functionals.

	B3LYP			BHLYP		
ArEEAr	[c] C_1	[c] C_2	C_3	C_1	C_2	C_3
Si[a]	0.9717	0.0047	0.0041	0.9219	0.0083	0.0048
Ge[a]	0.9768	0.0046	0.0039	0.9328	0.0049	0.0043
Sn[a]	0.9770	0.0052	0.0026	0.9380	0.0064	0.0027
Pb[b,c,d]						

[a] Ar'= C_6H_3-2,6(C_6H_3-2,6-iPr_2)$_2$.
[b] Ar*= C_6H_3-2,6(C_6H_2-2,4,6-iPr_3)$_2$.
[c] See eq (19)
[d]Too large for hybride SF-CV(2)-DFT calculation

Table S6 Contributions to the singlet [c] Ψ_{SF}^{S} wave function from a SF-CV(2)-DFT calculation on the liner Ar'EEAr' (E=Si,Ge,Sn) and Ar*PbPbAr* sytems based On BP86 calculations

	BP86		
ArEEAr	C_1	C_2	C_3
Si[a]	0.9551	0.0350	0.0015
Ge[a]	0.9410	0.0479	0.0031
Sn[a]	0.7601	0.2149	0.0151
Pb[b]	0.0333	0.9327	0.0175

[a] Ar'= C_6H_3-2,6(C_6H_3-2,6-iPr_2)$_2$.

[b] Ar*= C_6H_3-2,6(C_6H_2-2,4,6-iPr_3)$_2$.

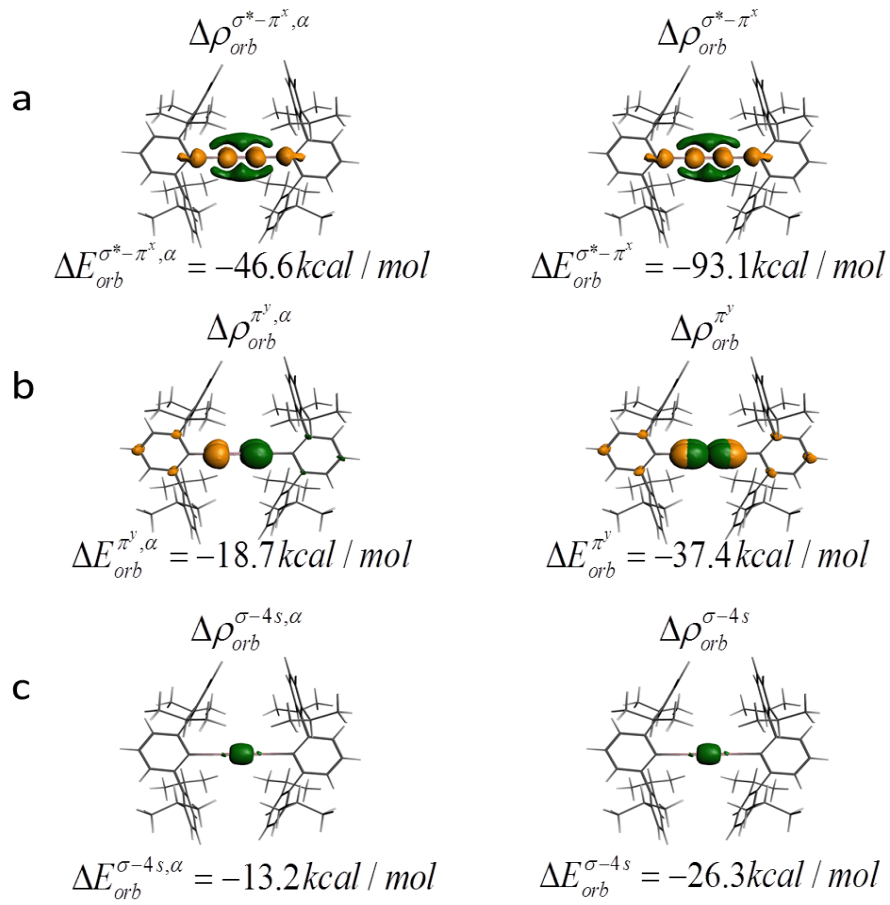

Figure S1. NOCV deformation densities for the linear silicon compound based on doublet fragments. (a) Contours of σ^*/π^x-NOCV deformation density with the corresponding energy contributions. The contour values are 0.003 au. (b) Contours of π^y-NOCV deformation density with the corresponding energy contributions. The contour values are 0.003 au. (c) Contours of σ-NOCV deformation density with the corresponding energy contributions. The contour values are 0.002 au. Green represents positive contours and orange negative contours.

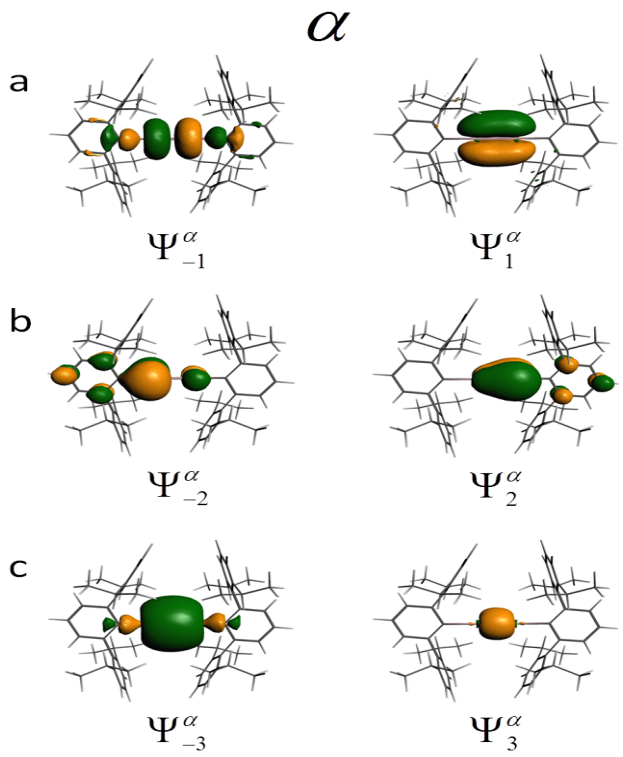

Figure S2. NOCV's for linear Si compound with doublet fragments.

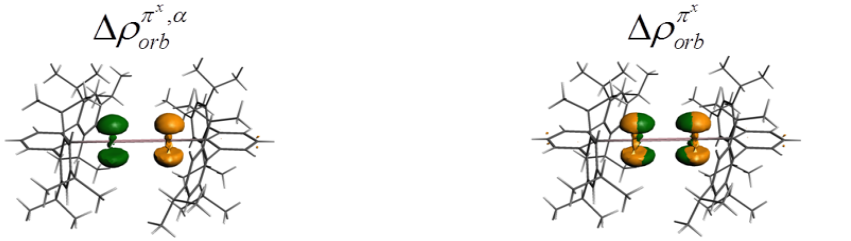

$\Delta E_{orb}^{\pi^x,\alpha} = -14.1 kcal/mol$ $\Delta E_{orb}^{\pi^x} = -28.2 kcal/mol$

Figure S3. NOCV deformation densities for the linear lead compound based on doublet fragments. Contours of the π^x -NOCV deformation density with the corresponding energy contributions. The contour values are 0.003 au. Green represents positive contours and orange negative contours.